



Cite this: DOI: 10.1039/d5lp00191a

Variation of refractive indices in self-assembling honeycomb patterned PMMA films

Mohamed Rishard Rameez,^a AbdulRahman Ghannoum,^b Kissan Mistry,^c Omar Awad, Kevin Musselman and Patricia Nievea *^d

A novel solvent casting method for poly methyl methacrylate (PMMA) thin films which allows for morphology and refractive index manipulation is presented in this work. The effect of solvent casting on the morphology and the optical properties of PMMA is studied as a function of solute concentration and the casting relative humidity. Acetic acid is used as the PMMA solvent and is presented as an alternative to toluene, tetrahydrofuran, and chloroform. Casted PMMA films annealed with relative humidities above 30% showed self-assembled nonporous honeycomb patterns. The refractive index of the cast films was observed to decrease from 1.49 to 1.41 as the casting relative humidity increased from 20% to 100%. Optical microscopic images revealed that the concentration of PMMA in the solution is strongly correlated to the size of honeycombs in the pattern. The depth of the honeycombs decreased from 3000 nm to 400 nm as the annealing relative humidity increased from 20% to 100%. Whereas the diameter of the honeycombs increased from 0.75 mm to 2.7 mm with increasing PMMA concentration. These results demonstrate the ability to produce PMMA thin films with specific structural dimensions and optical properties using acetic acid, which can be used to modify surfaces for various sensing applications.

Received 26th June 2025,
Accepted 21st October 2025

DOI: 10.1039/d5lp00191a
rsc.li/rscapplpolym

Introduction

Poly(methyl methacrylate) (PMMA) is a widely used polymer known for its exceptional optical transparency, lightweight nature, and high impact resistance, making it a preferred material in various scientific and industrial applications, including optics, electronics, and biomedicine.^{1–3} PMMA has been used in many applications, which include pneumatic actuation, analytical separation, conductive devices, optical devices, sensors, medical applications, polymer electrolytes, polymer viscosity control, and drug delivery.^{4–13} Most of these applications utilize a solution containing PMMA to perform various types of surface modifications (*i.e.* adhesion, coating, painting, polymer mixing, film casting *etc.*).¹⁴ While PMMA's versatility can be further enhanced through additives,² its processing and film-forming properties are significantly influenced by the choice of solvent and casting conditions. For many applications, PMMA in powder or pellet form is usually dissolved in a solvent. Traditional solvents such as toluene, dichloromethane, and chloroform have been extensively used in PMMA thin-film fabrication; however, their impact on film

morphology and optical characteristics depends on many factors such as casting temperature and casting concentration causing variations from that of the bulk.^{15,16} Recent studies have also shown that PMMA-based thin films can respond significantly to post-treatment in different solvent atmospheres, such as water/acetone/methanol systems, which influence their morphology, roughness, and refractive index.¹⁷ These observations highlight the sensitivity of PMMA films to solvent environment and motivate the search for alternative, less hazardous processing routes. Despite these advancements, alternative solvents with potential benefits, such as acetic acid, remain largely unexplored.

Acetic acid is a strong, colorless, organic solvent commonly used in the dissolution of inorganic acids and bases.¹⁸ Previous studies have demonstrated that acetic acid can influence mechanical properties, crystallinity, and surface morphology in polyhydroxybutyrate, suggesting its potential applicability to other polymer systems.¹⁹ Additionally, research has shown that the morphology of PMMA films can be controlled by adjusting casting temperature and relative humidity (RH), leading to the formation of porous honeycomb patterns.²⁰ According to M. Hernández-Guerrero *et al.* these patterns emerge through breath figures, where the solvent evaporation in extremely humid conditions causes water droplets in the air to condense on the sample in a self-ordered manner creating a template.²⁰ As the droplets evaporate, they leave behind voids, resulting in an organized porous polymer surface. In this

^aZown, North York, ON, M2N 7E7, Canada

^bDepartment of Chemical Engineering, Qatar University, P.O. Box 2713, Doha, Qatar

^cApple, One Apple Park Way, Cupertino, CA 95014, USA

^dDepartment of Mechanical and Mechatronics Engineering, University of Waterloo, Waterloo, Ontario, N2L 3G1, Canada. E-mail: pnievea@uwaterloo.ca



study, we build upon the findings of M. Hernández-Guerrero *et al.*; however, instead of forming porous honeycomb patterns, our method produces PMMA films with irregular non-porous honeycomb structures.

Zhou *et al.* previously reported the formation of nonporous honeycomb-patterned PMMA films using tetrahydrofuran as a weak organic solvent.^{21,22} However, the physical and optical properties of these films have not been extensively studied, nor has the effect of different humidity levels been thoroughly investigated.

In this study, we investigate the use of 99% glacial acetic acid as a solvent in preparing PMMA solutions for thin-film casting at various humidity levels, with a particular focus on the complex morphology and optical properties of the resulting films. PMMA concentrations in the solvent were varied between 1–10 wt% since solutions exceeding 10% PMMA were found to be too viscous for effective casting. The prepared solutions were then drop-cast onto silicon substrates in a chamber where the temperature was fixed and the relative humidity was controlled from 20% to 100% RH. The morphology of the annealed films was studied using an optical microscope and a 3D optical profilometry, while their optical properties were characterized through reflectometry.

Experimental section

Materials

Atactic poly methyl methacrylate (PMMA) powder with an approximate molecular weight of 15 000 (11335038, Fisher scientific) was dissolved in HPLC grade 99% glacial acetic acid (A35500, Fisher Scientific) to form the casting solution. Si wafers with 3" diameters and 500 μm thicknesses (477, University Wafer) with a native oxide were used as the casting substrates. Wafers were cleaned following the RCA-1 process. In this process a solution containing 65 ml of 27% ammonium hydroxide (05730, ProChem Inc.), 65 ml of 30% hydrogen peroxide (H325100, Fisher Scientific) and 325 ml DI water was prepared. This solution was then heated to 70 °C and the wafers were soaked in the solution for 15 minutes. Finally, the wafers were washed using DI water and dried with a flow of nitrogen gas.

Solution preparation

PMMA was weighed and dispensed into a glass vial. Glacial acetic acid was then dispensed into the vial using a micropipette while monitoring the mass using a scale in order to determine the concentration of PMMA in the casting solution. For the given molecular mass of PMMA, a maximum of 10 wt% solution was determined to be appropriate since higher concentrations formed visible suspensions of PMMA that precipitated in the casting solution. Therefore, 1, 5, and 10 wt% samples were prepared. In order to promote the dissolution of PMMA in acetic acid, a stir bar was introduced. The vial containing the solution was stirred for 4 hours to ensure complete dissolution.

Drop casting and curing

Thin PMMA films on silicon wafers were achieved through drop casting using a micropipette. About 100 μL of the PMMA solution was used per wafer. Samples were cured in a humidity and temperature controlled stainless steel chamber. Continuous flow of humid air through the chamber allowed for humidity control. Humid air with RH ranging from 20%–100% was prepared by bubbling dry air through water at different flow rates. The humidity was verified using an Omega humidity sensor positioned at the inlet. The chamber was placed on top of a hotplate set to 60 °C to maintain a constant rate of solvent evaporation. The wafers with casted PMMA were held under these conditions for 30 minutes and then air dried and annealed at 250 °C to ensure complete film curing. A total of nine PMMA samples were prepared and then cured at different humidity levels.

Reflectometry

Reflectance spectra of the cured PMMA samples were obtained using a reflectometer (Filmetrics F40). The spectra were measured in the visible light range (500–850 nm). A model consisting of three layers (air-PMMA-silicon substrate) was set in the FILMeasure analysis software to determine the unknown film thickness and refractive index. The Cauchy optical dispersion model²² was used to fit the refractive index to the measured reflectance spectrum. The Cauchy model is used for transparent material to determine an empirical relationship between the refractive index and wavelength, as such the extinction coefficient (k) is set to zero in this model. An initial guess for the refractive index was set to 1.4 based on expected PMMA refractive index values from literature.²³ Values for the initial guess were varied until a goodness of fit (GOF) equal to or larger than 99% was achieved. To improve accuracy, backside reflection was included in the model. The model is only fitted between the wavelengths ranging from 500–850 nm. This was done to avoid regions with lower signal to noise ratios (*i.e.*, 400–500 nm). Higher concentrations of PMMA were found to produce thicker films causing more light diffraction, which would require longer wavelengths (*i.e.*, infrared and beyond) when performing reflectometry. Thus, only the films produced using 1 wt% PMMA solutions were analyzed using reflectometry owing to reflectance efficiency.

Microscopic/SEM imaging

Optical microscopic images of the annealed films were taken at 2.5 \times magnification to study morphological variations. For surface analysis, a scanning electron microscope (SEM) (JEOL JSM-7200F) was used to produce images. The surface of the PMMA was sputter coated with iridium (4 nm thickness) to enhance conductivity at the surface of the sample.

3D profilometry

The 3D structure of the resulting films was analyzed using a BRUKER optical profiler to assess surface uniformity and topographical features. Samples cast using 1, 5, and 10 wt% PMMA

solutions were examined. The profiler provided quantitative measurements of surface roughness, allowing for comparison across different concentrations and insight into how polymer content influenced the film morphology.

Results and discussion

Morphology of the annealed films

Optical micrographs of PMMA films prepared using 1, 5 and 10 wt% PMMA solutions above 30% RH demonstrate a clear honeycomb pattern with varying sizes as seen in Fig. 1a–c. Similar morphologies were observed at higher RH as well. Films casted below 30% RH did not form any visible patterns,

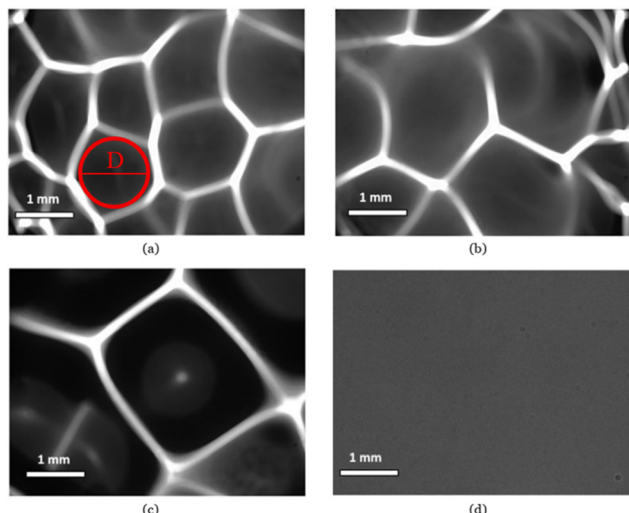


Fig. 1 Optical micrograph of PMMA thin films casted under 30% relative humidity using an acetic acid solution with (a) 1 wt% showing an example of a honeycomb cell diameter (*D*), (b) 5 wt% and (c) 10 wt% PMMA. (d) PMMA casted using 1 wt% PMMA solution under 20% relative humidity.

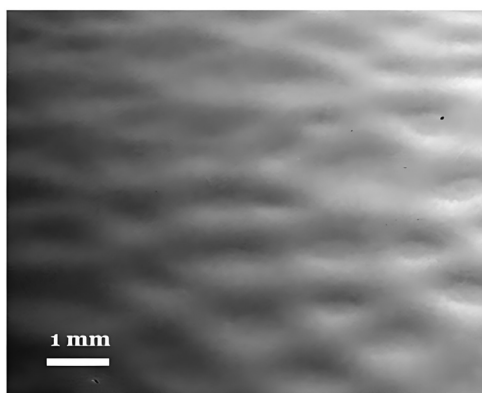


Fig. 2 Scanning electron micrograph of a PMMA thin film drop casted using an acetic acid solution with 1 wt% PMMA showing the morphology at the surface.

as seen for the film in Fig. 1d, which was 1 wt% PMMA solution casted at 20% RH. It is hence evident that the RH during drop casting is the main contributing factor for the formation of honeycomb patterns.

The diameter of a honeycomb cell is defined as that of the largest circle that can be inscribed within the polygonal opening, tangent to the inner walls without intersecting them, an example is shown in Fig. 1(a). The size of the honeycombs increased with increasing PMMA concentrations in the casting solution. The diameter of the honeycomb using a 1 wt%

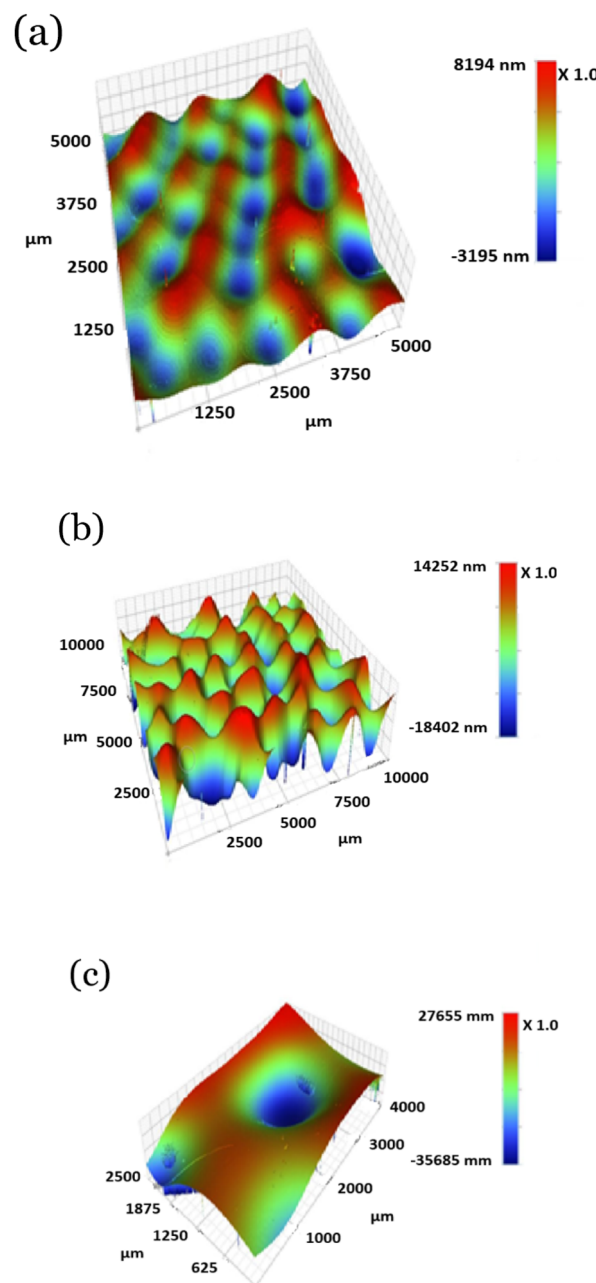


Fig. 3 Optical profilometer 3D surface topography of PMMA thin films showing different honeycomb patterns drop casted using (a) 1 wt% PMMA at 30% relative humidity, (b) 5 wt% PMMA at 30% relative humidity, (c) 10 wt% PMMA at 30% relative humidity.



PMMA solution ranged between 0.75–1.25 mm whereas the diameters for the 5 wt% PMMA and 10 wt% PMMA solutions ranged between 1.5–2.0 mm and 2.25–2.75 mm, respectively (see Fig. 1).

The presence of honeycomb patterns above 30% RH was also verified using SEM imaging at 25 \times magnification, which has a larger depth of field. Fig. 2 is an SEM image of a PMMA film made using 1 wt% PMMA solution casted at 30% RH. It clearly shows the morphology present at the surface of the PMMA films and the formation of hexagonal patterns. PMMA thin films prepared using other solvents (*i.e.*, dichloromethane and chloroform) have been reported to produce flat surfaces²⁴ but further testing with different levels of humidity may produce non-porous honeycomb patterns.

To further investigate the 3D structure of the prepared PMMA thin films a 3D profilometer was utilized to produce the images seen in Fig. 3. It can be seen from the 3D structure that the center of the honeycomb is curved inwards creating a crater on the surface of the film. The edges of the honeycomb patterns are slightly raised from the surface of the film, creating a hill/valley formation. The vertical ranges (*i.e.*, from minimum to maximum) of 1 wt%, 5 wt% and 10 wt% PMMA films were ± 4 μ m, ± 15 μ m and ± 32 μ m, respectively. This correlation demonstrates the ability to control the surface structure of PMMA thin films by manipulating the PMMA concentration in the drop casting solution.

Structural differences were also present when the RH was varied during casting, as seen in Fig. 4 and these patterns were

only observed through the optical profilometer. The recorded size variations in the hill/valley formations for casting in 30, 40, 50 and 60% RH were ± 4.3 μ m, ± 2.67 μ m, ± 1.65 μ m and ± 1.15 μ m, respectively. To address repeatability, the scans were repeated on multiple regions of each film and obtained consistent values within ± 0.2 μ m.

These results demonstrate that increasing the RH during drop casting increases the uniformity on the topology of the honeycomb structures. The results also suggest that increasing the RH decreases the diameter of the honeycomb pattern formed. This could be attributed to the influence of relative humidity on the balance between solvent evaporation and polymer solidification. At higher RH, adsorbed water molecules slow the evaporation of acetic acid and act as a plasticizer, reducing PMMA chain mobility. This prolongs the drying time and allows the polymer film to level more uniformly, which decreases both the depth of the honeycomb depressions and the effective diameter of the cells. Conversely, at lower RH, faster solvent removal and higher chain mobility lead to more rapid contraction of the polymer-rich regions, resulting in deeper honeycombs patterns with larger diameters. Overall, the effect of humidity is to regulate evaporation kinetics and chain relaxation, which in turn governs the final honeycomb morphology.

Refractive index and thickness of the films

The optical properties of the PMMA films were analyzed using reflectometry. As seen in Fig. 5, the model is fitted between the wavelengths ranging from 500–850 nm. Table 1 summar-

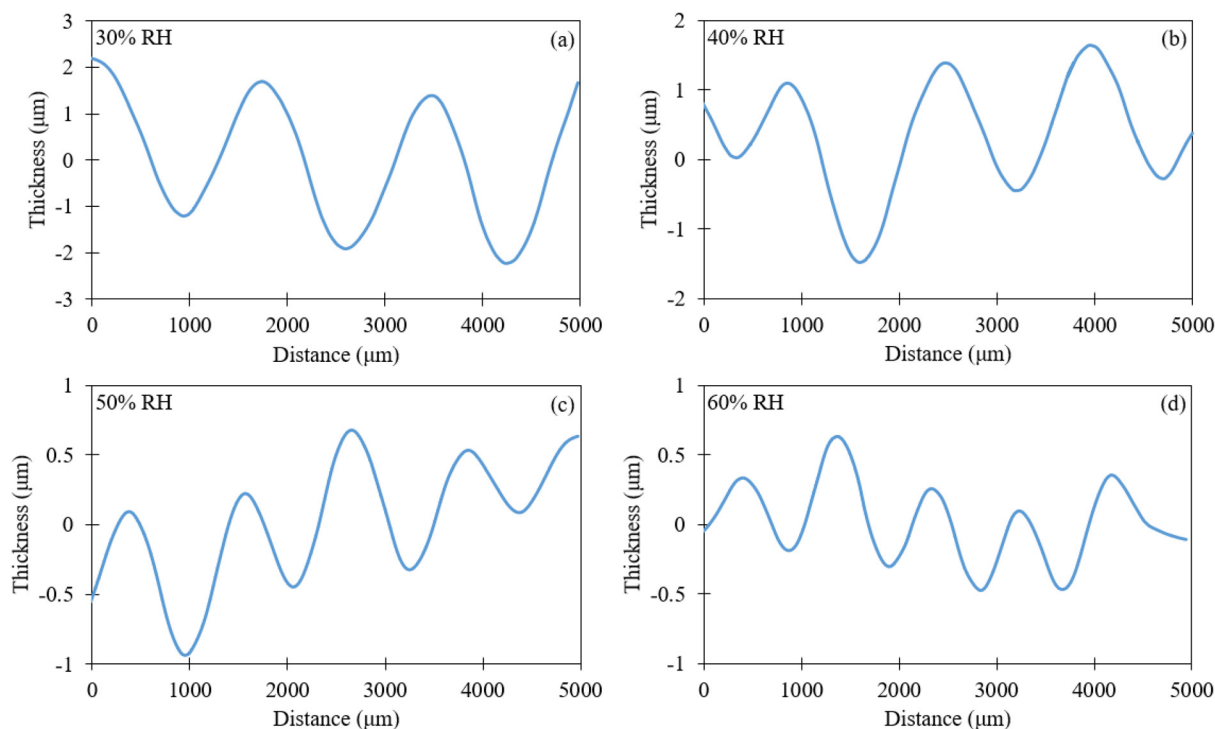


Fig. 4 Optical profilometer surface height profiles of PMMA thin films prepared using 1 wt% PMMA casting solution at (a) 30% RH, (b) 40% RH, (c) 50% RH and (d) 60% RH.



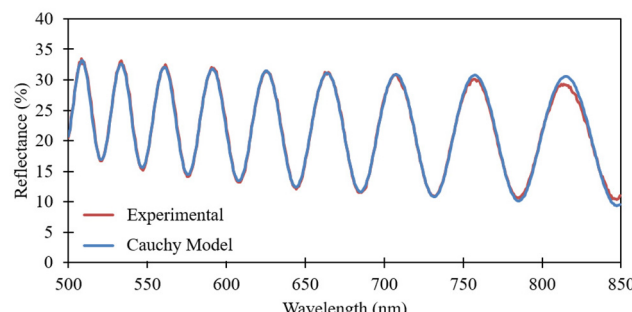


Fig. 5 Reflectance vs. wavelength – experimental and Cauchy model curve for the 1% wt/wt PMMA at 30% RH.

Table 1 Thickness and the GOF derived from the model fit for 1% wt/wt PMMA with varying RH

| RH (%) | Thickness (nm) | GOF |
|--------|----------------|--------|
| 20 | 3082 | 0.998 |
| 30 | 3594 | 0.9974 |
| 40 | 2713 | 0.9979 |
| 50 | 3527 | 0.999 |
| 60 | 2811 | 0.992 |
| 70 | 3828 | 0.9973 |
| 80 | 3379 | 0.9968 |
| 90 | 2598 | 0.992 |
| 100 | 3933 | 0.9984 |

izes the thicknesses and the goodness of fit of the modeled spectrum for the nine different samples measured. While the model provides an effective or average film thickness, it does not fully capture the exact topographical variations observed experimentally.

As shown in Table 1, the predicted film thicknesses are on the order of 3 microns, whereas profilometry measurements for the 1 wt% PMMA sample at 30% RH revealed surface features, hills and valleys, reaching up to 4 microns in height. This discrepancy is expected, as the model assumes an idealized, perfectly flat PMMA film, while actual films often vary in uniformity due to roughness and/or texture variations occurring during the fabrication process. Hence, further studies would need to consider the limitations of this modeling approach by taking into account the effects of PMMA film uniformity.

Once the goodness of fit was above 99%, the refractive index, n , was extracted. Fig. 6 shows the variation in refractive indices of the PMMA films at different casting RH levels *versus* wavelength. The refractive index is observed to decrease with increasing casting RH.

The observed decrease is gradual until about 60% RH where larger drops in the refractive index are seen (*i.e.*, change between 60–70% and 70–80% RH). All curves of the refractive indices relative to wavelength followed the same trend for PMMA recorded in literature.²³ As seen in Fig. 7, the refractive index change with wavelength for PMMA cured under 20% RH is similar to earlier observations of PMMA.²³ The morphology of the films fabricated at casting RH levels less than 30% were

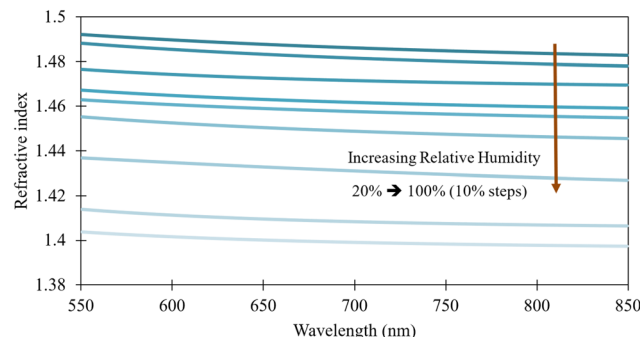


Fig. 6 Variation of refractive index of PMMA with respect to casting relative humidity vs. wavelength – Cauchy model.

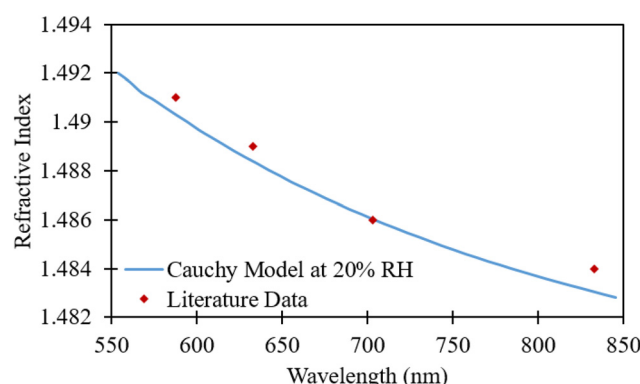


Fig. 7 Variation in refractive index of PMMA cast at 20% relative humidity compared to the variation of the bulk.

similar to that of the bulk PMMA and thus its refractive index. Therefore, these results show that the refractive indices of PMMA films produced using acetic acid at RH levels higher than 30% result in significant variation in refractive indices.

This variation in refractive index can be attributed to the same humidity-driven mechanisms that influence film morphology and mentioned earlier. At low RH, faster solvent removal leads to rapid solidification and tighter packing of polymer-rich regions, producing deeper honeycomb depressions and a higher effective density, which corresponds to a higher refractive index. At higher RH, adsorbed water slows evaporation and plasticizes the PMMA, allowing the surface to relax more uniformly; this increases free volume and reduces the effective density, leading to a lower refractive index. The absence of droplet templating explains the nonporous nature of the films, while humidity-dependent evaporation kinetics and chain relaxation account for both the observed changes in the morphology and refractive index.

Conclusions

This paper has presented a novel method for fabricating nonporous honeycomb patterned PMMA thin films using acetic acid as a solvent. In this method, acetic acid evaporates slowly



and does not induce water droplet templating, in contrast to the rapid solvent evaporation method reported in ref. 20. Thus, the solvent-rich regions retract unevenly during drying, while the polymer-rich phase solidifies. This process at the liquid–air interface produces ridges and depressions, but without a droplet lattice to guide the arrangement. As a result, the patterns are nonporous and relatively irregular.

The ability to control the honeycomb pattern size and optical properties by adjusting PMMA concentration and casting relative humidity (RH) provides a precise way to design films with specific characteristics for sensing applications. By increasing the PMMA concentration from 1 wt% to 10 wt%, the honeycomb diameter was tuned from 0.75 mm to 2.7 mm, demonstrating that the pattern size can be directly controlled to optimize surface area for sensor interaction. Additionally, the observed refractive index tuning (1.49–1.41) is within the range that significantly modifies optical confinement in waveguide sensors, suggesting strong potential for integration into optical sensing platforms. Ongoing work explores this application in coated optical fibers.

Comparison of experimental measurements with a Cauchy optical dispersion model used to fit the refractive index to the measured reflectance spectrum show a great degree of agreement, despite fabrication variations on the PMMA film surface roughness not considered in the model. Varying the RH from 20% to 100% also provided a control over the depth of the honeycomb structure from 3000 nm to 400 nm, enabling the customization of the film's mechanical and optical properties. This is critical for designing sensors with enhanced responsiveness to environmental changes. The depth of the pattern influences the film's interaction with light and can be optimized for specific sensing applications, such as detection of small shifts in refractive index or changes in light intensity caused by the presence of analytes.

This method's precision in controlling structural and optical properties makes it a promising technique for the development of highly sensitive optical sensors, such as those used for detecting gases, biomolecules, or pollutants. The ability to fabricate these films with a high degree of reproducibility and control over key parameters directly translates to more reliable and adaptable sensing platforms. As such, the proposed method provides a robust approach for fabricating PMMA films tailored for advanced sensing applications, where both structural and optical properties must be finely tuned to achieve the required sensor characteristics.

Author contributions

The manuscript was written through contributions of all authors. All authors have given approval to the final version of the manuscript.

Conflicts of interest

There are no conflicts to declare.

Abbreviations

| | |
|------|------------------------------|
| PMMA | Poly(methyl methacrylate) |
| RH | Relative humidity |
| GOF | Goodness of fit |
| SEM | Scanning electron microscopy |

Data availability

The data supporting this article have been included as part of the supplementary information (SI). Supplementary information: SEM and profilometry images; modelling and experimental data. See DOI: <https://doi.org/10.1039/d5lp00191a>.

Acknowledgements

This research was supported by the Natural Sciences and Engineering Research Council of Canada (NSERC), Discovery Grant RGPIN-2017-05026.

References

- 1 H. Lacroix, *Thermohydroelastic Properties of Polymethylmethacrylate*, Koninklijke Philips Electronics N. V., Philips Research Europe, PR-TN 2007/00440, 2007.
- 2 M. M. Demir, M. Memesa, P. Castignolles and G. Wegner, PMMA/Zinc Oxide Nanocomposites Prepared by *In situ* Bulk Polymerization, *Macromol. Rapid Commun.*, 2006, 27(10), 763–770, DOI: [10.1002/marc.200500870](https://doi.org/10.1002/marc.200500870).
- 3 R. Q. Frazer, R. T. Byron, P. B. Osborne and K. P. West, PMMA: An Essential Material in Medicine and Dentistry, *J. Long-Term Eff. Med. Implants*, 2005, 15(6), 629–639, DOI: [10.1615/jlongtermeffmedimplants.v15.i6.60](https://doi.org/10.1615/jlongtermeffmedimplants.v15.i6.60).
- 4 H. Hashim, N. I. Adam, N. H. M. Zaki, Z. S. Mahmud, C. M. S. Said, M. Z. A. Yahya and A. M. M. Ali, Natural Rubber-Grafted with 30% Poly(Methylmethacrylate) Characterization for Application in Lithium Polymer Battery, in *2010 International Conference on Science and Social Research (CSSR 2010)*, 2010, pp. 485–488. DOI: [10.1109/CSSR.2010.5773825](https://doi.org/10.1109/CSSR.2010.5773825).
- 5 A. C. Henry, T. J. Tutt, M. Galloway, Y. Y. Davidson, C. S. McWhorter, S. A. Soper and R. L. McCarley, Surface Modification of Poly(Methyl Methacrylate) Used in the Fabrication of Microanalytical Devices, *Anal. Chem.*, 2000, 72(21), 5331–5337, DOI: [10.1021/ac0006851](https://doi.org/10.1021/ac0006851).
- 6 L.-H. Lee and W.-C. Chen, High-Refractive-Index Thin Films Prepared from Trialkoxysilane-Capped Poly(Methyl Methacrylate)-Titania Materials, *Chem. Mater.*, 2001, 13(3), 1137–1142, DOI: [10.1021/cm000937z](https://doi.org/10.1021/cm000937z).
- 7 J. J. Shah, J. Geist, L. E. Locascio, M. Gaitan, M. V. Rao and W. N. Vreeland, Surface Modification of Poly(Methyl Methacrylate) for Improved Adsorption of Wall Coating

Polymers for Microchip Electrophoresis, *Electrophoresis*, 2006, **27**(19), 3788–3796, DOI: [10.1002/elps.200600118](https://doi.org/10.1002/elps.200600118).

8 B. Adhikari and S. Majumdar, Polymers in Sensor Applications, *Prog. Polym. Sci.*, 2004, **29**(7), 699–766, DOI: [10.1016/j.progpolymsci.2004.03.002](https://doi.org/10.1016/j.progpolymsci.2004.03.002).

9 A. Isha, N. A. Yusof, M. Ahmad, D. Suhendra, W. M. Z. W. Yunus and Z. Zainal, A Chemical Sensor for Trace V(v) Ion Determination Based on Fatty Hydroxamic Acid Immobilized in Polymethylmethacrylate, *Sens. Actuators, B*, 2006, **114**(1), 344–349, DOI: [10.1016/j.snb.2005.06.007](https://doi.org/10.1016/j.snb.2005.06.007).

10 J. Kost and R. Langer, Responsive Polymeric Delivery Systems, *Adv. Drug Delivery Rev.*, 2012, **64**, 327–341, DOI: [10.1016/j.addr.2012.09.014](https://doi.org/10.1016/j.addr.2012.09.014).

11 D. T. Beruto, R. Botter and M. Fini, The Effect of Water in Inorganic Microsponges of Calcium Phosphates on the Porosity and Permeability of Composites Made with Polymethylmethacrylate, *Biomaterials*, 2002, **23**(12), 2509–2517, DOI: [10.1016/S0142-9612\(01\)00385-4](https://doi.org/10.1016/S0142-9612(01)00385-4).

12 M. Shi, J. D. Kretlow, P. P. Spicer, Y. Tabata, N. Demian, M. E. Wong, F. K. Kasper and A. G. Mikos, Antibiotic-Releasing Porous Polymethylmethacrylate/Gelatin/Antibiotic Constructs for Craniofacial Tissue Engineering, *J. Controlled Release*, 2011, **152**(1), 196–205, DOI: [10.1016/j.jconrel.2011.01.029](https://doi.org/10.1016/j.jconrel.2011.01.029).

13 S. Mishra and G. Sen, Microwave Initiated Synthesis of Polymethylmethacrylate Grafted Guar (GG-g-PMMA), Characterizations and Applications, *Int. J. Biol. Macromol.*, 2011, **48**(4), 688–694, DOI: [10.1016/j.ijbiomac.2011.02.013](https://doi.org/10.1016/j.ijbiomac.2011.02.013).

14 S. Bistac and J. Schultz, Solvent Retention in Solution-Cast Films of PMMA: Study by Dielectric Spectroscopy, *Prog. Org. Coat.*, 1997, **31**(4), 347–350, DOI: [10.1016/S0300-9440\(97\)00093-3](https://doi.org/10.1016/S0300-9440(97)00093-3).

15 N. Patra, M. Salerno, A. Diaspro and A. Athanassiou, Effect of Solvents on the Dynamic Viscoelastic Behavior of Poly(Methyl Methacrylate) Film Prepared by Solvent Casting, *J. Mater. Sci.*, 2011, **46**(15), 5044–5049, DOI: [10.1007/s10853-011-5424-9](https://doi.org/10.1007/s10853-011-5424-9).

16 N. Patra, A. C. Barone and M. Salerno, Solvent Effects on the Thermal and Mechanical Properties of Poly(Methyl Methacrylate) Casted from Concentrated Solutions, *Adv. Polym. Technol.*, 2011, **30**(1), 12–20, DOI: [10.1002/adv.20203](https://doi.org/10.1002/adv.20203).

17 C. Geiger, J. Reitenbach, L. P. Kreuzer, T. Widmann, P. Wang, R. Cubitt, C. Henschel, A. Laschewsky, C. M. Papadakis and P. Müller-Buschbaum, PMMA-b-PNIPAM Thin Films Display Cononsolvency-Driven Response in Mixed Water/Methanol Vapors, *Macromolecules*, 2021, **54**(7), 3517–3530, DOI: [10.1021/acs.macromol.1c00021](https://doi.org/10.1021/acs.macromol.1c00021).

18 I. M. Kolthoff and A. Willman, The Dissociation of Some Inorganic Acids, Bases and Salts in Glacial Acetic Acid as Solvent.1 I, *J. Am. Chem. Soc.*, 1934, **56**(5), 1007–1013, DOI: [10.1021/ja01320a002](https://doi.org/10.1021/ja01320a002).

19 P. Anbukarasu, D. Sauvageau and A. Elias, Tuning the Properties of Polyhydroxybutyrate Films Using Acetic Acid via Solvent Casting, *Sci. Rep.*, 2015, **5**(1), 1–14, DOI: [10.1038/srep17884](https://doi.org/10.1038/srep17884).

20 M. Hernández-Guerrero and M. H. Stenzel, Honeycomb Structured Polymer Films via Breath Figures, *Polym. Chem.*, 2012, **3**(3), 563–577, DOI: [10.1039/C1PY00219H](https://doi.org/10.1039/C1PY00219H).

21 X. D. Zhou, S. C. Zhang, W. Huebner, P. D. Ownby and H. Gu, Effect of the Solvent on the Particle Morphology of Spray Dried PMMA, *J. Mater. Sci.*, 2001, **36**(15), 3759–3768, DOI: [10.1023/A:1017982018651](https://doi.org/10.1023/A:1017982018651).

22 M. Quinten, *A Practical Guide to Optical Metrology for Thin Films*, John Wiley & Sons, 2012.

23 N. Sultanova, S. Kasarova and I. Nikolov, Dispersion Properties of Optical Polymers, *Acta Phys. Pol. A*, 2009, **116**(4), 585–587, DOI: [10.12693/APhysPolA.116.585](https://doi.org/10.12693/APhysPolA.116.585).

24 E. Mohajerani, F. Farajollahi, R. Mahzoon and S. Bagheri, Morphological and thickness analysis for PMMA spin coated films, *J. Optoelectron. Adv. Mater.*, 2007, **9**, 3901–3906.

